International Journal of Pharmaceutics 402 (2010) 103–109

Contents lists available at ScienceDirect

International Journal of Pharmaceutics

journal homepage: www.elsevier.com/locate/ijpharm

Development and evaluation of a monolithic drug-in-adhesive patch for valsartan

Naohiro Nishida[a,*], Kazuhiro Taniyama[b], Toshihiro Sawabe[b], Yoichi Manome[b]

[a] Pharmaceutical Technology Research Laboratories, R&D Dept., TOA EIYO Ltd., 1 Tanaka, Yuno, Iizaka, Fukushima-shi, Fukushima 960-0280, Japan
[b] Fukushima Research Laboratories, R&D Dept., TOA EIYO Ltd., 1 Tanaka, Yuno, Iizaka, Fukushima-shi, Fukushima 960-0280, Japan

ARTICLE INFO

Article history:
Received 24 May 2010
Received in revised form 31 August 2010
Accepted 27 September 2010
Available online 7 October 2010

Keywords:
Drug-in-adhesive patch
Valsartan
Diisooctyl sodium sulfosuccinate
Yucatan micro pig
Transdermal

ABSTRACT

The purpose of this study was to investigate the feasibility of a monolithic drug-in-adhesive (DIA) patch as a transdermal therapeutic system for the administration of valsartan (VAL). To improve the penetration of VAL in the patch, several chemical penetration enhancers were investigated by *in vitro* hairless mouse and Yucatan micro pig (YMP) skin permeation studies. A combination of isopropyl myristate (IPM)/diisooctyl sodium sulfosuccinate (AOT) most strongly enhanced the permeation of VAL. Since the concentration of VAL through the patch in hairless rat (HR) *in vivo* was correlated with that in HR skin *in vitro*, VAL that permeated through the skin could effectively pass into the systemic circulation. The plasma concentration–time profile of VAL after the patch was applied in humans was estimated by a convolution technique from the results of the *in vitro* YMP study, which indicated that the concentration of VAL could be sufficient to produce a pharmacological effect. These results demonstrate that the combination of IPM/AOT may be useful for the development of a practical DIA patch for VAL.

1. Introduction

Valsartan (VAL) is a highly selective angiotensin II type 1 receptor blocker that has been widely used for the treatment of hypertension. When administrated orally in humans, VAL is rapidly absorbed. Its maximum concentration (C_{max}) occurs at 2–4 h (Cyong and Uebara, 1998), and it is then excreted into bile (Israili, 2000). VAL is not metabolized by cytochrome P450 (Israili, 2000) and is mostly excreted without metabolic conversion (Brookman et al., 1997). The bioavailability (BA) of VAL is 10–35% (Israili, 2000). This low BA of VAL is mainly due to poor absorption in the gastrointestinal tract, which is mainly attributed to the ionized tetrazole and/or carboxyl group of VAL (Fig. 1) in the tract. Additionally, food intake is known to reduce the C_{max} and AUC of VAL by 50% and 40%, respectively (Israili, 2000), which may reduce its pharmacological effect. Therefore, if we can improve the BA of VAL and minimize the effect of food intake, we should be able to confer further therapeutic benefits to hypertensive patients. The transdermal administration of VAL is a possible solution to overcome these problems.

A transdermal route offers many advantages for the local and systemic delivery of a drug: avoidance of a first-pass effect, prolongation of the plasma concentration and pharmacological action, reduced frequency of side effects associated with other administration routes, and rapid elimination from the blood by simple removal. A variety of transdermal therapeutic systems (TTS), such as cream, gel, patches and physical devices, have been used for the treatment of diseases. With regard to transdermal application for systemic drug delivery, a patch is the most convenient formulation in terms of productivity, manufacturing cost and practical usability. Transdermal patches can be classified into three types: monolithic or multilaminate drug-in-adhesive (DIA), liquid reservoir and polymer matrix. A monolithic DIA-type patch is easy to use and consists of a parent drug, additives, pressure–sensitive–adhesive (PSA), backing film and release liner. Over the past few decades, only a limited number of drugs have been successfully delivered via a TTS, since most drugs cannot penetrate the skin due to the barrier function of the stratum corneum (SC). Various methodologies, including both chemical and physical approaches, have been investigated to improve the skin permeation of drugs. The use of chemical penetration enhancers (CPE) has been mostly considered for the development of efficient monolithic DIA-type patches.

We examined the effects of CPEs in a VAL suspension or solution on the permeation of VAL through the skin of the hairless mouse (HM). We found that isopropyl myristate (IPM), *n*-octyl-ß-D-thioglucoside (OTG) and diisooctyl sodium sulfosuccinate (AOT) were potent candidates among the CPEs screened (see Supplemental table and figure). IPM is well-known to be an effective CPE for a wide variety of drugs including indapamide (Ren et al., 2009), *S*-amlodipine (Sun et al., 2009), isosorbide dinitrate (Myoung and Choi, 2002), lincomycin hydrochloride (Panigrahi et al., 2006) and terbutaline sulfate (Panigrahi et al., 2005). OTG is a non-ionic surfactant and membrane protein solubilizer that is known to enhance the skin permeation of peptides such as eel cal-

* Corresponding author. Tel.: +81 24 542 3171; fax: +81 24 542 3205.
E-mail address: nisida.naohiro@toaeiyo.co.jp (N. Nishida).

0378-5173/$ – see front matter © 2010 Elsevier B.V. All rights reserved.
doi:10.1016/j.ijpharm.2010.09.031

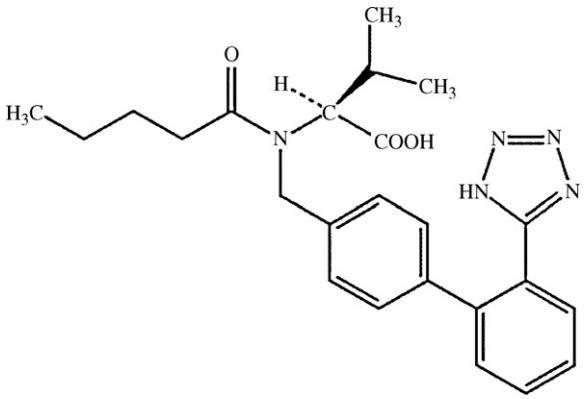

Fig. 1. Chemical structure of valsartan.

citonin, ebiratide (Ogiso et al., 1991, 1994a,b) and ketotifen (Murthy and Vishwanath, 2006). AOT is an anionic surfactant that is known to improve the skin permeation of nitroglycerin (Varshney et al., 1999) and 5-fluorouracil (Gupta et al., 2005). Although many potent CPEs have been reported based on *in vitro* studies, the enhancement effects were often overestimated due to the influence of solvents, and thus it has been difficult to predict these effects in PSA such as a patch formulation (Cho and Choi, 1998; Myoung and Choi, 2002). Moreover, HM skin is more permeable than human skin or human-equivalent skin (Bronaugh et al., 1982; Ghosh et al., 2000; Roy et al., 1994; Scott et al., 1986). Therefore, even if we were to identify the most potent CPEs in an *in vitro* system based on a solution formulation, these results would be unreliable for achieving an optimal formulation for the development of a TTS patch.

In the present study, we focused on the feasibility of a monolithic DIA patch containing VAL with the three above-mentioned CPEs: IPM, OTG and AOT. Various combinations of CPEs in both suspension and patch formulations of VAL were assessed by both HM skin and Yucatan micro pig (YMP) skin permeation studies *in vitro*. The pharmacokinetic profile of the optimized VAL patch was clarified by permeation studies in hairless rat (HR) *in vivo* and *in vitro*. Finally, the plasma concentration–time curve of VAL in humans with this patch was estimated by a convolution technique based on *in vitro* YMP skin permeation data.

2. Materials and methods

2.1. Materials

VAL was purchased from Sequoia Research Product Ltd. (Oxfordshire, UK). Gelva® multipolymer resin solution 1753 (GMS1753) was obtained from Solutia Inc. (MO, USA). IPM and AOT (Aerosol® OT; diisooctyl sodium sulfosuccinate) were purchased from Wako Pure Chemical Industries Ltd. (Osaka, Japan). Tris (2,4-pentanedionato) aluminum (III) (Al-AA) and OTG were obtained from DOJINDO LABORATORIES (Kumamoto, Japan). All other reagents and solvents were of analytical grade.

2.2. Animals

HM (HR-1, 20–30 g, 6 weeks, male) was purchased from Hoshino Laboratory Animals Inc. (Ibaragi, Japan). HR (HWY, 200–240 g, 6 weeks, male) was purchased from Japan SLC Inc. (Shizuoka, Japan). Frozen YMP skins (whole skin, 5 months, female) were purchased from Charles River Laboratories Japan (Kanagawa, Japan). Animals had free access to food and water until the experiments. YMP skin was stored at −80 °C until the preparation of dermatomes. All of the animal experimental protocols were in accordance with the guidelines of the committee for animal experimentation at Toa Eiyo Ltd.

2.3. Preparation of skin

2.3.1. HM and HR skin

After HM or HR was scarified with diethyl ether, full-thickness skin was surgically excised. Subcutaneous fat and capillary blood vessels were carefully removed with a scalpel and surgical scissors (Agrawala and Ritschel, 1988; Cho and Choi, 1998). The excised skin was cut to an appropriate size and placed in phosphate buffered saline (PBS) for a while. In the preparation of stripped skin (Flynn et al., 1981), the SC of the excised skin was stripped 20 times by the application of tape (Scotch® tape MP-18, Sumitomo 3 M Limited, Japan).

2.3.2. Dermatomed YMP skin

After frozen YMP skin was thawed at room temperature, subcutaneous fat was carefully removed with a scalpel and surgical scissors. The dermis side was cut to adjust the total skin thickness to 500 μm with a vibratome (VIB3000Plus, MEIWAFOSIS Co., Ltd., Japan). The skin was cut to an appropriate size and frozen at −80 °C until the experiment.

2.4. Preparation of the suspension formulation and solubility measurement

VAL and CPE were added to vehicles in the ratios shown in Table 1(a) and the mixtures were stirred for 48 h at 25 °C using a mechanical stirrer (SW-M60, NISSIN, Japan). The mixture was then centrifuged at 9000 × *g* and the supernatant was filtered with a 0.45 μm PTFE membrane filter. One millilitre of filtered solution was transferred into a 100 mL measuring flask, and methanol was added to make up a 100 mL solution. The concentration of VAL in the solution was measured by high-performance liquid chromatography (HPLC).

2.5. Preparation of the patch formulation

The formulations of the prepared patches are summarized in Table 1(b). Patches were prepared by the solvent evaporation technique. After weighed amounts of VAL, CPE, IPM and Al-AA were dissolved in methanol, PSA solution (i.e., GMS1753) was added to the above solution and mixed with a pencil mixer. The mixed solution was cast at a thickness of 400 μm on a polyester backing membrane (ESTER FILM E5100, TOYOBO Co., Ltd., Japan) with corona treatment using a laboratory coating applicator (COATMASTER 509 MC-I, ERICHSEN GmbH & Co., KG, Germany), and dried in an oven at 60 °C for 1 h to remove residual organic solvents. Finally, the dried PSA layer with a thickness of about 100 μm was laminated with polyester release liner (ESTER FILM E7006, TOYOBO Co., Ltd., Japan) with silicone treatment. The patch was stored at ambient temperature until further study.

2.6. In vitro skin permeation study

2.6.1. Experimental procedure

An *in vitro* skin permeation study was performed using a vertical Franz-type glass diffusion cell system with a magnetic stirrer, a thermostatic water bath and an auto-sampler (Microetter®, Hanson Research Corporation, USA). Each diffusion cell with a water jacket was connected to a thermostatic water bath at 37 ± 1 °C, and maintained at 37 ± 1 °C by circulating water from the bath. This ensured that the skin surface temperature was maintained at 32 ± 1 °C. The receptor chamber of the diffusion cell (volume of 7 mL

Table 1
Suspension formulations.

Formulation	VAL (%)	OTG (%)	AOT (%)	Water (%)	IPM (%)	Enhancer(s)	Drug in suspension (mg/0.5 mL)	Saturated solubility (mg/mL)
(a)								
S1	1			99		None	About 5.0	0.17 ± 0.04
S2	1				99	Single	About 5.0	2.74 ± 0.05
S3	1	3			96	Binary	About 5.0	3.21 ± 0.08
S4	1		3		96	Binary	About 5.0	7.80 ± 0.12

Formulation[a]	VAL (%)	OTG (%)	AOT (%)	IPM (%)	PSA[b] (%)	Enhancer(s)	Drug content (mg/1.3 cm^2)
(b)							
T1	10				89.5	None	1.72 ± 0.20
T2	10			50	39.5	Single	2.04 ± 0.01
T3	10	3			86.5	Single	1.68 ± 0.10
T4	10		3		86.5	Single	1.74 ± 0.21
T5	10	3		50	36.5	Binary	2.43 ± 0.18
T6	10		3	50	36.5	Binary	2.35 ± 0.08

[a] Including Al-AA 0.5% as a cross-linker.
[b] PSA; GMS1753.

and an effective diffusion area of 1.3 cm^2) was filled with PBS and stirred at 600 rpm during the experiment.

The excised skin was mounted on the top of the diffusion cell, fastened with a rigid clamp and left for about 1 h to hydrate before the experiment was started. After 0.5 mL of suspension or 1.3 cm^2 of patch was applied to the SC side of the skin, 1 mL of solution in the receptor chamber was collected as the sample and the same volume of fresh PBS was immediately added back to it at a predetermined time (for suspension formulation; 0, 1, 2, 3, 4, 5, 6, 7 and 8 h, for patch formulation; 0, 2, 4, 6, 8, 12, 16, 20, 24, 30, 36 and 48 h). The concentration of VAL in samples was determined by HPLC.

2.6.2. Determination of VAL by HPLC

The concentration of VAL was measured by HPLC (LC-2010C Chromatograph, SHIMADZU CORPORATION, Japan). A C18 ODS column (COSMOSIL 5C18-AR-II 4.6 mm I.D. × 150 mm, Nacalai Tesque Inc., Japan) was maintained at 40 °C. The mobile phase was maintained at pH 2.2 with a mixture of 15 mM dihydrogen potassium phosphate aqueous solution/acetonitrile (45/55) and pumped at a flow rate of 1 mL/min. The injection volume was 10 μL. The wavelength of the UV detector was 225 nm. The retention time of VAL was about 4.0 min.

2.6.3. Data analysis

The cumulative amount of VAL that permeated per unit of skin surface area (Q) was plotted against time. The permeation profile was fitted to Eq. (1) (Diez et al., 1991; Scheuplein, 1967);

$$Q = KLC_v \left(\frac{D}{L^2}t - \frac{1}{6} - \frac{2}{\pi^2} \sum_{n=1}^{\infty} \frac{(-1)^n}{n^2} \exp\left(\frac{-Dn^2\pi^2 t}{L^2} \right) \right) \quad (1)$$

where C_v is the drug concentration in the donor vehicle, K is the SC/vehicle partition coefficient, D is the diffusion coefficient in the skin barrier (i.e., SC) and L is the thickness of the skin barrier (i.e., SC). P_1 and P_2 are defined as follows:

$$P_1 = \frac{D}{L^2} \quad (2)$$

$$P_2 = KLC_v \quad (3)$$

These parameters were obtained from curve-fitting, and the flux and lag time were then calculated as follows:

$$\text{Flux} = P_1 P_2 = \frac{KC_v D}{L} \quad (4)$$

$$\text{Lag time} = \frac{1}{6P_1} \frac{L^2}{6D} \quad (5)$$

2.7. In vivo HR absorption study

2.7.1. Experimental procedure

A prepared patch with 12 cm^2 was applied to the back of HR. Blood samples (0.2 mL each) were collected from the jugular vein at predetermined times (0, 1, 2, 4, 6, 8, 10, 12 and 24 h) using a heparinized syringe and kept on ice until they were centrifuged at 14,000 × g for 10 min at 4 °C. The obtained plasma samples were stored at −30 °C until the analyses. Aliquots (50 μL) of plasma samples were transferred to a 96-well plate, and 50 μL of distilled water, 50 μL of internal standard (dexamethasone) and 250 μL of acetonitrile were then added. After the samples were centrifuged at 1000 × g for 20 min at 4 °C, the supernatants were diluted 2-fold by distilled water and subjected to LC/MS/MS analyses. The lower limit of quantification was 1 ng/mL with a precision of 10.3% and an accuracy of 11.1%. The calibration curve was linear over a concentration range of 1–1000 ng/mL. The imprecision of the assay did not exceed 9.48% following the analysis of VAL. The inaccuracy of VAL did not exceed −10.9% to 4.73%. The overall recovery of VAL from rat plasma exceeded 80%.

2.7.2. Determination of VAL in plasma by LC/MS/MS

The concentration of VAL in a plasma sample was determined using a Waters® ACQUITY™ Ultra Performance LC system consisting of a Binary Solvent Manager, Sample Manager and TQ Detector. As a UPLC column, a Waters® ACQUITY UPLC BEH® C18 (2.1 mm × 50 mm, 1.7 μm) column with a Van Guard BEH® C18 (2.1 mm × 5 mm, 1.7 μm) pre-column was used, and this was maintained at 40 °C. The mobile phase consisted of a mixture of A (water)/B (0.1%, v/v, formic acid in acetonitrile) and was pumped at a flow rate of 0.4 mL/min according to the following multistep gradients: (Step 1) a 1.5 min linear gradient to 100% mobile phase B, (Step 2) a 1.2 min isocratic elution in 100% mobile phase B, (Step 3) a 0.01 min linear gradient to 0% mobile phase B, and (Step 4) a 0.29 min isocratic elution in 100% mobile phase A. The run-time was 3 min. The injection volume was 5 μL. The MS/MS conditions were as follows: ionization method was electrospray ionization (ESI), scan mode was multiple reaction monitoring (MRM), ionization voltage was 3500 V, ionization source temperature was 130 °C, cone gas was N_2, cone gas flow rate was 50 L/h, desolvation gas was N_2, desolvation gas flow rate was 900 L/h, collision gas was Ar, and collision gas flow rate was 0.25 mL/min. MRM was set at 436.25 to 291.20 m/z for VAL and at 393.22 to 355.29 m/z for the internal standard. The system was controlled by Masslynx™ software.

Table 2
Skin permeation parameters of VAL from suspension formulations through excised HM skin. Each value represents the mean ± SD of three experiments.

Formulation	Flux (μg/cm²/h)	Lag time (h)	Relative γ_s (–)
S1	0.4 ± 0.2	5.0 ± 2.1	1.000
S2	10.2 ± 5.7*	3.1 ± 0.2	0.071
S3	239.5 ± 119.9***	3.9 ± 0.2	0.002
S4	288.0 ± 51.9***	1.4 ± 0.1**	0.005

* $p < 0.05$ vs. S1 (Dunnett's multiple comparison test with one-way ANOVA).
** $p < 0.01$ vs. S1 (Dunnett's multiple comparison test with one-way ANOVA).
*** $p < 0.001$ vs. S1 (Dunnett's multiple comparison test with one-way ANOVA).

2.7.3. Data analysis

Measured plasma concentrations were used to determine the maximum plasma concentration (C_{max}), time to reach C_{max} (T_{max}) and area under the plasma concentration–time curve (AUC_t) by the model-independent analysis method. The pharmacokinetic parameters were calculated using WinNonlin ver. 2.1 (CA, USA).

2.8. Prediction of plasma concentration

The *in vitro* skin permeation data were analyzed numerically by a convolution technique (Eq. (6)) to clarify the plasma concentration–time profile after patch application.

$$C(t) = \int_0^t F(\theta)G(t-\theta)d\theta \quad (6)$$

where $C(t)$, F and G are the plasma concentration as a function of time, the input into the system (i.e., *in vitro* skin permeation data) and the unit impulse response (i.e., intravenous data), respectively.

2.9. Statistical analysis

Dunnett's multiple comparison test with one-way analysis of variance (ANOVA) or Student's *t*-test was performed to determine the significance of differences among formulations using EXSUS ver. 7.5.2 based on SAS release 9.1.3 (CAC Corp., Osaka, Japan and SAS Institute Japan Ltd., Tokyo, Japan). A value of $p < 0.05$ was considered to be significant.

3. Results and discussions

3.1. Effects of CPEs in suspension formulations

The effects of CPEs on the permeation of VAL from suspension formulations (S1–S4) (Table 1(a)) through excised HM skin are summarized in Table 2. The permeations with IPM (S2–S4) were significantly higher ($p < 0.05$ or $p < 0.001$) than that with water (S1). The addition of OTG (S3) and AOT (S4) enhanced permeation by about 25-fold compared to that with IPM alone (S2).

If a drug is saturated in a vehicle that does not affect the skin, its thermodynamic activity in the vehicle is maximal, which leads to a constant flux value that is independent of the type of vehicle. This relationship can be described as follows (Higuchi, 1960):

$$\frac{dQ}{dt} = \frac{KC_vDA}{L} = \frac{a_vDA}{\gamma_sL} \quad (7)$$

$$\gamma_s = \frac{\gamma_v}{K} \quad (8)$$

where K is the SC/vehicle partition coefficient, C_v is the saturated solubility in the donor vehicle, D is the diffusion coefficient in the skin barrier, A is the effective diffusion area, L is the thickness of the skin barrier, a_v is the thermodynamic activity in the donor vehicle, γ_s is the activity coefficient in the skin barrier and γ_v is the activity coefficient in the donor vehicle. While VAL was saturated in all of the suspension formulations, the flux values in S2–S4 were significantly higher than that in S1. According to analyses based on Eqs. (7) and (8), the γ_s coefficients of VAL with IPM (S2), IPM/OTG (S3) and IPM/AOT (S4) were significantly decreased compared to that with water (S1) (Table 2). The rank order of the decrease in these coefficients was as follows: IPM/OTG (S3) > IPM/AOT (S4) > IPM (S2). Generally, a decrease in the γ_s coefficient is associated with an increase in the penetrant solubility in SC. Therefore, IPM, IPM/OTG and IPM/AOT may decrease the barrier function of SC, and lead to enhanced drug solubility in SC. OTG and AOT may work in cooperation with IPM to decrease the barrier function and/or increase the partition into the SC layer.

3.2. Effects of CPEs in patch formulations

Various patches (T1–T6) with or without the above three CPEs were prepared as described in Table 1(b). The effects of CPEs on the permeation of VAL from the patch through excised HM skin are summarized in Table 3. In intact skin, systems with a single enhancer, IPM (T2), OTG (T3) and AOT (T4), significantly improved the permeation of VAL ($p < 0.05$ or 0.01) compared to the system with no enhancer (T1). System with two enhancers, IPM/OTG (T5) and IPM/AOT (T6), significantly enhanced the permeation ($p < 0.001$) compared to the other systems (T1–T4). The highest permeation was observed with T6, which had a flux value of 134.0 ± 11.2 μg/cm²/h and a lag time of 3.1 ± 0.2 h. In stripped skin without an SC layer, IPM (T2), IPM/OTG (T5) and IPM/AOT (T6) significantly enhanced permeation to a similar extent ($p < 0.001$), whereas the addition of OTG (T3) or AOT (T4) without IPM had little effect on permeation compared to the system with no enhancer (T1). These results suggest the following possible mechanisms of enhancement: (1) IPM interacted with not only SC but also viable epidermis and this enhancement effect extended to both layers and (2) OTG and AOT only interacted with SC, and thus these enhancement effects were limited in SC.

Table 3
Effects of CPEs on the permeation of VAL from prepared patches (T1–T6) through excised HM skin. Each value represents the mean ± SD of three experiments.

Formulation[a]	Intact skin		Stripped skin	
	Flux[b] (μg/cm²/h)	Lag time[b] (h)	Flux[b] (μg/cm²/h)	Lag time[b] (h)
T1, without (control)	0.3 ± 0.0 (1)	10.9 ± 0.8 (1.0)	29.2 ± 0.9 (1)	1.0 ± 0.0 (1.0)
T2, IPM 50%	18.2 ± 2.4** (61)	10.5 ± 0.8 (1.0)	141.3 ± 24.9*** (5)	1.2 ± 0.0** (1.0)
T3, OTG 3%	5.1 ± 0.3* (17)	11.8 ± 0.6 (1.1)	32.3 ± 0.5 (1)	1.0 ± 0.0 (1.0)
T4, AOT 3%	9.6 ± 0.1* (32)	11.6 ± 0.1 (1.1)	35.9 ± 6.6 (1)	1.0 ± 0.1 (1.0)
T5, IPM 50%/OTG 3%	79.2 ± 8.0*** (264)	3.1 ± 0.2*** (0.3)	174.8 ± 27.9*** (6)	1.2 ± 0.0** (1.2)
T6, IPM 50%/AOT 3%	134.0 ± 11.2*** (447)	3.1 ± 0.2*** (0.3)	196.3 ± 32.1*** (6)	1.2 ± 0.1** (1.2)

[a] VAL 10%, IPM, OTG or AOT (see table), Al-AA (cross-linker) 0.5%, GMS1753 up to 100%.
[b] Values in parentheses represent the ratio vs. T1.
* $p < 0.05$ vs. T1 (Dunnett's multiple comparison test with one-way ANOVA).
** $p < 0.01$ vs. T1 (Dunnett's multiple comparison test with one-way ANOVA).
*** $p < 0.001$ vs. T1 (Dunnett's multiple comparison test with one-way ANOVA).

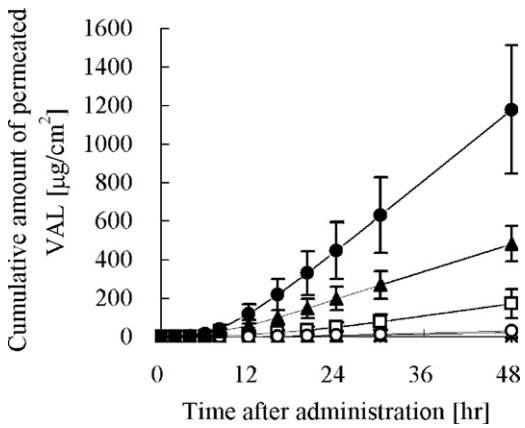

Fig. 2. Permeation profiles of VAL from prepared patches (T1–T6) through excised YMP skin. Each value represents the mean ± SD of three experiments. The symbols represent (*; T1), (□; T2), (Δ; T3), (○; T4), (▲; T5) and (●; T6), respectively.

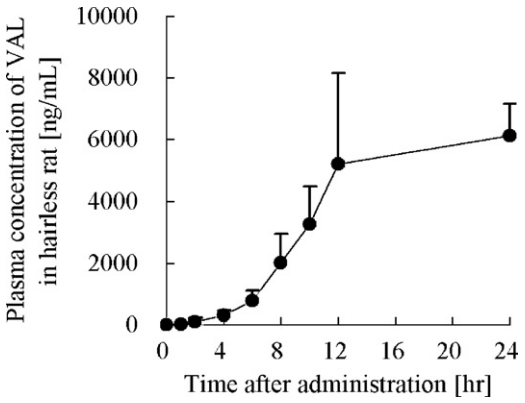

Fig. 3. Time-course of the mean plasma concentration of VAL in HR after the transdermal administration of a prepared patch (T6). Each value represents the mean ± SD of three experiments.

It is well known that the permeation of drugs through HM skin is considerably greater than that through human skin (Bronaugh et al., 1982; Ghosh et al., 2000; Roy et al., 1994; Scott et al., 1986), which leads to an overestimation of the plasma concentration in humans via transdermal administration. Therefore, YMP skin, which has a structure similar to that of human skin, has been used to obtain a better estimation of drug permeation in humans. Fig. 2 and Table 4 show the permeation profiles of VAL from the prepared patches (T1–T6) through excised YMP skin. In all cases, steady-state permeation was observed from 24 to 48 h. While a slight but significant increase in permeation ($p < 0.05$) was observed with the addition of OTG (T3) or AOT (T4), further increases ($p < 0.05$, $p < 0.01$ or 0.001) were found with IPM (T2), IPM/OTG (T5) and IPM/AOT (T6) compared to the system with no enhancer (T1). In particular, the system with two enhancers, IPM/OTG (T5) and IPM/AOT (T6), showed significantly enhanced permeation compared to the system without IPM (T1). A synergistic effect on skin permeation was found with the addition of 3% of OTG or AOT to IPM. As a possible explanation for the increased permeation in T5 and T6 compared to that in T2, OTG and AOT are thought to synergistically enhance the permeation with IPM. The mechanism by which IPM enhances permeation is considered be associated with increased lipid fluidity in the skin through the disruption of lipid packing due to high affinity between IPM and components in the skin (Benson, 2005; Liron and Cohen, 1984; Panigrahi et al., 2005; Sloan et al., 1986; Sun et al., 2009; Walker and Smith, 1996). On the other hand, OTG and AOT enhance permeation by reducing the barrier of the SC (Ogiso et al., 1994a; Varshney et al., 1999). Therefore, the partition of OTG or AOT into the SC is promoted by IPM in T5 or T6, respectively, which means that high concentrations of these surfactants penetrate the skin and show a greater enhancing effect than the corresponding systems without IPM (T3 or T4). These binary systems, T5 and T6, also show a significant decrease in lag time compared to the system with no enhancer (T1) ($p < 0.01$ or $p < 0.001$). The highest permeation was observed in T6, with a flux of 34.3 ± 10.1 μg/cm²/h and a lag time of 10.8 ± 0.7 h (Table 4).

In a comparison of the *in vitro* studies with HM and YMP skin, permeation rates through YMP skin were much lower than those through HM skin. The flux in YMP skin was decreased 10 to 26% and the lag time was increased about 1.4- to 3.5-fold compared to that in HM skin, which suggests that the permeation barrier of YMP skin was considerably high, similar to that of human skin. The enhancement of VAL permeation by the above three enhancers was confirmed in suspension with HM skin and in patch formulations with both HM and YMP skin.

3.3. *In vitro/in vivo correlation in HR*

The pharmacokinetic profile of VAL administered transdermally by a prepared patch (T6) with an area of 12 cm² (VAL 21.7 ± 0.72 mg/12 cm²) was clarified by *in vivo* HR absorption and *in vitro* HR skin permeation studies. The plasma concentration–time profile of VAL after patch application in HR *in vivo* is shown in Fig. 3. The concentration of VAL gradually increased from 0 to 12 h and remained at a constant level from 12 to 24 h. The C_{max}, T_{max} and AUC values were 7280 ± 979 ng/mL, 20.0 ± 6.9 h and 86,200 ± 19,340 ng h/mL, respectively. To clarify the time-dependent cumulative permeated amount of VAL in HR *in vivo*, the profile was analyzed by a deconvolution technique as follows (Loo

Table 4
Effects of CPEs on the permeation of VAL from prepared patches (T1–T6) through excised YMP skin. Each value represents the mean ± SD of three experiments.

Formulation[a]	YMP		vs. HM[c]	
	Flux[b] (μg/cm²/h)	Lag time[b] (h)	Flux (fold)	Lag time (fold)
T1, without (control)	0.05 ± 0.0 (1)	20.3 ± 1.9 (1.0)	0.17	1.9
T2, IPM 50%	3.9 ± 1.9* (78)	15.5 ± 3.3 (0.8)	0.21	1.4
T3, OTG 3%	0.8 ± 0.3* (16)	19.4 ± 3.2 (1.0)	0.16	1.6
T4, AOT 3%	1.0 ± 0.5* (20)	18.5 ± 2.0 (0.9)	0.10	1.6
T5, IPM 50%/OTG 3%	13.0 ± 2.6** (260)	8.9 ± 1.6*** (0.4)	0.16	2.9
T6, IPM 50%/AOT 3%	34.3 ± 10.1*** (686)	10.8 ± 0.7** (0.5)	0.26	3.5

[a] VAL 10%, IPM, OTG or AOT (see table), Al-AA 0.5%, GMS1753 up to 100%.
[b] Values in parentheses represent the ratio vs. T1.
[c] Flux and lag time for YMP were divided by the corresponding values for HM.
* $p < 0.05$ vs. T1 (Dunnett's multiple comparison test with one-way ANOVA).
** $p < 0.01$ vs. T1 (Dunnett's multiple comparison test with one-way ANOVA).
*** $p < 0.001$ vs. T1 (Dunnett's multiple comparison test with one-way ANOVA).

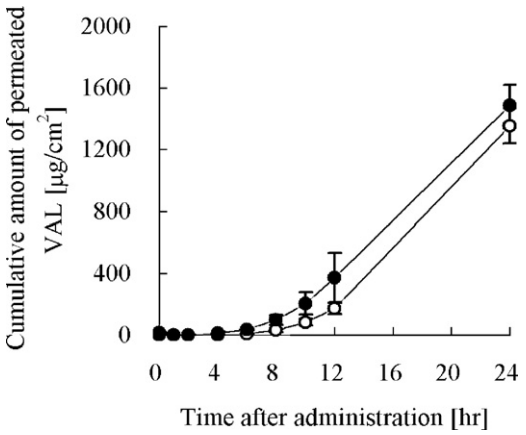

Fig. 4. *In vivo* (●) and *in vitro* (○) permeation profiles of VAL from a prepared patch (T6) through HR skin. Each value represents the mean ± SD of three experiments.

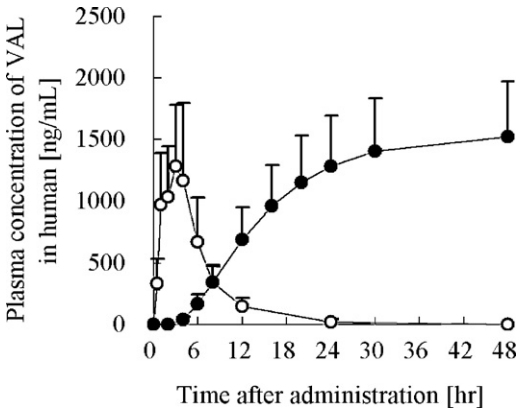

Fig. 5. Time-course of the mean plasma concentration of VAL after transdermal (●, T6 with an area of 100 cm² (mean ± SD, $n = 3$)) and oral (○, VAL 40 mg p.o. (mean ± SD, $n = 6$)) administration.

and Riegelman, 1968):

$$\frac{A_T}{A_\infty} = \frac{C(T) + k_{el}\int_0^T C(t)dt + ((X_P)_T/V_C)}{k_{el}\int_0^\infty C(t)dt} \quad (9)$$

where $C(T)$ is the plasma concentration at $t = T$, k_{el} is the elimination rate constant, V_C is the volume of distribution in the central compartment and $(X_P)_T$ is the amount of drug in the peripheral compartment at $t = T$. The cumulative amount of absorbed VAL from $t = 0$ to $t = T$ (i.e., A_T) is assumed to be the cumulative amount of VAL permeated through HR skin. The obtained permeation profile was fitted to Eq. (1) and the skin permeation parameters were calculated by Eqs. (2)–(5). The *in vivo* and *in vitro* permeation profiles of VAL are compared in Fig. 4. While the *in vivo* lag time was slightly shorter than that *in vitro*, the *in vivo* profile of the time-dependent cumulative amount of VAL was not greatly different from that *in vitro*. The *in vivo* flux and lag time were 93.1 ± 4.6 μg/cm²/h and 8.0 ± 1.9 h, while those *in vitro* were 98.5 ± 7.7 μg/cm²/h and 10.3 ± 0.3 h, respectively. There was no significant difference (Student's *t*-test) between these corresponding parameters. These results indicate that the *in vivo* profile of VAL is consistent with the *in vitro* profile, and VAL that permeates through the skin effectively passes into the systemic circulation.

3.4. Prediction of the plasma concentration in humans

The most important goal in the development of TTS is to achieve a reliable estimation of the plasma concentration–time profile in humans after transdermal administration and to evaluate whether this concentration reaches a therapeutic level. Since YMP skin has a structure similar to that of human skin (Fujii et al., 1997; Godin and Touitou, 2007; Ngawhirunpat et al., 2004), based on the results of our YMP skin study, the plasma concentration–time profile of VAL in humans after the transdermal administration of a T6 patch with an area of 100 cm² was estimated by the convolution technique. The profiles with transdermal and oral administration (VAL 40 mg p.o.) are compared in Fig. 5. The pharmacokinetic data for VAL were obtained from a phase I clinical trial in Japan, which was described in detail in a local Japanese journal (Cyong and Uebara, 1998). Orally administrated VAL is known to be rapidly absorbed, and showed a C_{max} of 1373 ± 534 ng/mL at a T_{max} of 2.8 ± 1.0 h. Meanwhile, when VAL is administered transdermally, it can be absorbed gradually, and a C_{max} was estimated to be 1535 ± 192 ng/mL at a T_{max} of 48 h. This value is almost the same (about 1.64 mg/mL) as the therapeutically effective plasma concentration of VAL (Rizwan et al., 2008). The AUC value for the transdermal administration (49,960 ± 15,916 ng h/mL) was estimated to be about 6-fold greater ($p < 0.001$, Student's *t*-test) than that with oral administration (8883 ± 4022 ng h/mL). The relative bioavailability of VAL after transdermal administration vs. oral administration was calculated as follows:

$$F = \frac{AUC_{transdermal}Dose_{oral}}{AUC_{oral}Dose_{transdermal}} \quad (10)$$

The bioavailability of VAL administered transdermally with a T6 patch may be 1.6-fold greater than that with oral administration. As shown in Fig. 5, the plasma concentration after transdermal administration reached the C_{max} of oral administration and remained at a constant level for at least 24 h, which suggests a prolonged pharmacological effect compared to oral administration.

4. Conclusions

In the present study, we developed a monolithic DIA patch for VAL that incorporated IPM/AOT, and evaluated its potency. IPM/AOT had a synergistic effect on the permeation of VAL through both HM and YMP skin compared to each CPE alone. The permeation through HR skin *in vitro* and *in vivo* was correlated, suggesting that VAL that permeated through the skin could effectively pass into the systemic circulation. The plasma concentration in humans was estimated from an *in vitro* YMP skin permeation study: it reached a therapeutic range and remained at a constant level for at least 24 h. These results demonstrate the feasibility of a monolithic DIA patch for VAL with an IPM/AOT system. Further studies will be needed to fully elucidate the possibility of developing a VAL transdermal patch.

Appendix A. Supplementary data

Supplementary data associated with this article can be found, in the online version, at doi:10.1016/j.ijpharm.2010.09.031.

References

Agrawala, P., Ritschel, W.A., 1988. Influence of 1-dodecylhexahydro-2H-azepin-2-one (Azone) on the in vitro permeation of verapamil hydrochloride across rat, hairless mouse, and human cadaver skin. J. Pharm. Sci. 77, 776–778.

Benson, H.A., 2005. Transdermal drug delivery: penetration enhancement techniques. Curr. Drug Deliv. 2, 23–33.

Bronaugh, R.L., Stewart, R.F., Congdon, E.R., Giles Jr., A.L., 1982. Methods for in vitro percutaneous absorption studies. I. Comparison with in vivo results. Toxicol. Appl. Pharmacol. 62, 474–480.

Brookman, L.J., Rolan, P.E., Benjamin, I.S., Palmer, K.R., Wyld, P.J., Lloyd, P., Flesch, G., Waldmeier, F., Sioufi, A., Mullins, F., 1997. Pharmacokinetics of valsartan in patients with liver disease. Clin. Pharmacol. Ther. 62, 272–278.

Cho, Y.J., Choi, H.K., 1998. Enhancement of percutaneous absorption of ketoprofen: effect of vehicles and adhesive matrix. Int. J. Pharm. 169, 95–104.

Cyong, J.C., Uebara, K., 1998. Phase I study of angiotensin II receptor antagonist. CGP 48933 (Valsartan) – Single administration study, vol. 14, pp. 1703–1725.
Diez, I., Colom, H., Moreno, J., Obach, R., Peraire, C., Domenech, J., 1991. A comparative in vitro study of transdermal absorption of a series of calcium channel antagonists. J. Pharm. Sci. 80, 931–934.
Flynn, G.L., Durrheim, H., Higuchi, W.I., 1981. Permeation of hairless mouse skin II: membrane sectioning techniques and influence on alkanol permeabilities. J. Pharm. Sci. 70, 52–56.
Fujii, M., Yamanouchi, S., Hori, N., Iwanaga, N., Kawaguchi, N., Matsumoto, M., 1997. Evaluation of Yucatan micropig skin for use as an in vitro model for skin permeation study. Biol. Pharm. Bull. 20, 249–254.
Ghosh, B., Reddy, L.H., Kulkarni, R.V., Khanam, J., 2000. Comparison of skin permeability of drugs in mice and human cadaver skin. Indian J. Exp. Biol. 38, 42–45.
Godin, B., Touitou, E., 2007. Transdermal skin delivery: Predictions for humans from in vivo, ex vivo and animal models. Adv. Drug Deliv. Rev. 59, 1152–1161.
Gupta, R.R., Jain, S.K., Varshney, M., 2005. AOT water-in-oil microemulsions as a penetration enhancer in transdermal drug delivery of 5-fluorouracil. Colloids Surf. B: Biointerfaces 41, 25–32.
Higuchi, T., 1960. Physical chemical analysis of percutaneous absorption process from creams and ointments. J. Soc. Cosmet. Chem. 11, 85–97.
Israili, Z.H., 2000. Clinical pharmacokinetics of angiotensin II (AT1) receptor blockers in hypertension. J. Hum. Hypertens. 14, S73–S86.
Liron, Z., Cohen, S., 1984. Percutaneous absorption of alkanoic acids II: application of regular solution theory. J. Pharm. Sci. 73, 538–542.
Loo, J.C., Riegelman, S., 1968. New method for calculating the intrinsic absorption rate of drugs. J. Pharm. Sci. 57, 918–928.
Murthy, S.N., Vishwanath, B.A., 2006. N-octyl-beta-thioglucoside enhances the transdermal permeation of ketotifen. Pharmazie 61, 75–76.
Myoung, Y., Choi, H.K., 2002. Effects of vehicles and pressure sensitive adhesives on the penetration of isosorbide dinitrate across the hairless mouse skin. Drug Deliv. 9, 121–126.
Ngawhirunpat, T., Opanasopit, P., Prakongpan, S., 2004. Comparison of skin transport and metabolism of ethyl nicotinate in various species. Eur. J. Pharm. Biopharm. 58, 645–651.
Ogiso, T., Iwaki, M., Yoneda, I., Horinouchi, M., Yamashita, K., 1991. Percutaneous absorption of elcatonin and hypocalcemic effect in rat. Chem. Pharm. Bull. (Tokyo) 39, 449–453.
Ogiso, T., Paku, T., Iwaki, M., Tanino, T., 1994a. Mechanism of the enhancement effect of n-octyl-beta-D-thioglucoside on the transdermal penetration of fluorescein isothiocyanate-labeled dextrans and the molecular weight dependence of water-soluble penetrants through stripped skin. J. Pharm. Sci. 83, 1676–1681.
Ogiso, T., Paku, T., Iwaki, M., Tanino, T., Nishioka, S., 1994b. Percutaneous absorption of physiologically active peptides, ebiratide and elcatonin, in rats. Biol. Pharm. Bull. 17, 1094–1100.
Panigrahi, L., Ghosal, S.K., Pattnaik, S., 2006. Effect of permeation enhancers on the release and permeation kinetics of Lincomycin hydrochloride gel formulations through mouse skin. Indian J. Pharm. Sci. 68, 205–211.
Panigrahi, L., Pattnaik, S., Ghosal, S.K., 2005. The effect of pH and organic ester penetration enhancers on skin permeation kinetics of terbutaline sulfate from pseudolatex-type transdermal delivery systems through mouse and human cadaver skins. AAPS PharmSciTech 6, E167–E173.
Ren, C., Fang, L., Ling, L., Wang, Q., Liu, S., Zhao, L., He, Z., 2009. Design and in vivo evaluation of an indapamide transdermal patch. Int. J. Pharm. 370, 129–135.
Rizwan, M., Aqil, M., Ahad, A., Sultana, Y., Ali, M.M., 2008. Transdermal delivery of valsartan: I. Effect of various terpenes. Drug Dev. Ind. Pharm. 34, 618–626.
Roy, S.D., Hou, S.Y., Witham, S.L., Flynn, G.L., 1994. Transdermal delivery of narcotic analgesics: comparative metabolism and permeability of human cadaver skin and hairless mouse skin. J. Pharm. Sci. 83, 1723–1728.
Scheuplein, R.J., 1967. Mechanism of percutaneous absorption. J. Invest. Dermatol. 48, 79–88.
Scott, R.C., Walker, M., Dugard, P.H., 1986. A comparison of the in vitro permeability properties of human and some laboratory animal skins. Int. J. Cosmet. Sci. 8, 189–194.
Sloan, K.B., Koch, S.A., Siver, K.G., Flowers, F.P., 1986. Use of solubility parameters of drug and vehicle to predict flux through skin. J. Invest. Dermatol. 87, 244–252.
Sun, Y., Fang, L., Zhu, M., Li, W., Meng, P., Li, L., He, Z., 2009. A drug-in-adhesive transdermal patch for S-amlodipine free base: in vitro and in vivo characterization. Int. J. Pharm. 382, 165–171.
Varshney, M., Khanna, T., Changez, M., 1999. Effects of AOT micellar systems on the transdermal permeation of glyceryl trinitrate. Colloids Surf. B: Biointerfaces 13, 1–11.
Walker, R.B., Smith, E.W., 1996. The role of percutaneous penetration enhancers. Adv. Drug Deliv. Rev. 18, 295–301.